Study on the relationship between laser-induced damage threshold and microscopic properties of Ta_2O_5 films by the combination of experiment and simulation

CHENG XU[a,*], MING MA[a], HUANHUAN SUN[a], DI LIN[a], PEIZHONG FENG[a], JIANWEI QI[a], YINGHUAI QIANG[a], DAWEI LI[b], CHUNXIAN TAO[b]

[a]*School of Materials Science and Engineering, China University of Mining and Technology, Xuzhou 221116, China*
[b]*Key Laboratory of High Power Laser Materials, Shanghai Institute of Optics and Fine Mechanics, Chinese Academy of Sciences, Shanghai 201800, China*
[c]*School of Optics-Electrical and Computer Engineering, University of Shanghai for Science and Technology, Shanghai 200093, China*

Ta_2O_5 films were prepared by electron beam evaporation under different oxygen partial pressures. Three Ta_2O_5 models were constructed according to the experimental obtained O/Ta ratios to calculate the microscopic properties. It was shown that the oxygen vacancy significantly decreased the microscopic band gaps, which was due to the generation of a defect level in the energy gap formed by 5*d* state of tantalum. The LIDT shared the same trend with the microscopic band gaps. With the increase of the O/Ta ratios from 2.44 and 2.47 to 2.50, the LIDT increased by 62.2% and 54.7%, whereas the microscopic band gaps increased by 268% and 160%, respectively, compared to the initial value.

(Received September 28, 2015; accepted October 28, 2015)

Keywords: Ta_2O_5, Oxygen vacancy, Absorption, Laser damage

1. Introduction

The laser-induced damage of films has become one of the most important research focuses with the development of high-power laser systems. Many works have devoted to improving the laser-induced damage threshold (LIDT) and exploring the laser damage mechanism. It has been shown that the LIDT of films is connected with many parameters such as preparation methods, substrates, deposition conditions and post-processings [1-4]. The initiation factors in the laser-induced damage are related to substoichiometric defects, structural defects, impurities and so on [5]. It is concluded from the above that since the laser damage is very complicated, further studies are definitely of great necessity.

For the nanosecond laser damage, the effect of the band gap on the LIDT has always been ignored for a long time. It is mainly owing to the slight changes occurring on the band gap although the LIDT varies intensely [6-7]. In those studies, the band gap is usually fitted from the spectrum curve obtained by optical test and the light spot diameter of the test equipment is always on millimeter scale. Thus, this conventional band gap is also called as macroscopic band gap. Different from it, a new concept was brought out in our previous paper which was named as microscopic band gap [8]. It represents the band gap of very small area such as nanometer, which shows a good correlation with the LIDT. The possible reason is attributed to that the laser damage initiation is influenced strongly by the nano-area and even smaller area. Therefore, the properties of the nano-area such as the microscopic band gap may become more and more important to evaluate the laser damage resistance of the films. Base on this, we believe that it should be necessary and meaningful to do more studies on these microscopic properties.

In this paper, Ta_2O_5 films were prepared under different oxygen partial pressures. The optical properties, chemical composition, weak absorption and LIDT of the films were studied. According to the experimental obtained O/Ta ratios, different Ta_2O_5 models were constructed to calculate the microscopic properties including the microscopic band gap, partial density of state (PDOS) and charge density difference. An attempt was made firstly to explore the relationship between the LIDT and microscopic properties of Ta_2O_5 films.

2. Experimental

In the experiment, tetragonal Ta_2O_5 aggregates were used as the starting materials to prepare Ta_2O_5 films by electron beam evaporation method. Chemically treated and cleaned BK7 glasses were used as the substrates. In the deposition process, the oxygen partial pressures were kept

at 1.5×10^{-2} Pa and 2.5×10^{-2} Pa, respectively. The samples were denoted as A1 and A2. During the post-deposition process, both A1 and A2 were annealed at 673 K for 12 h. Transmittance spectra of the films were measured using a Lambda 900 spectrophotometer and the wavelength accuracy of the instrument during spectra recording was within 0.08%. The refractive indices and extinction coefficients were calculated by Essential Macleod (a thin film design software). The chemical composition of the films was analyzed by X-ray photoelectron spectroscopy (XPS) using focused (300 μm in diameter) monochromatic Al-Kα ($h\upsilon$=1486.6 eV) radiation. The Ar ions with the energy of 3 keV were used to etch to 10 nm beneath the film surface. The weak absorption was obtained by surface thermal lensing (STL) method, and the measurement accuracy was 1 ppm [9]. Laser damage testing was performed in the "1-on-1" regime according to ISO standard 11254-1, using 1064 nm Nd:YAG laser in single longitudinal mode with up to a 5 Hz repetition rate [10-11]. The LIDT was defined as the incident pulse energy density (J/cm^2) when the damage occurs at 0% damage possibility. In the simulation, Ta_2O_5 of the c12/c1 space group was used. The lattice constant were a = 12.7853 Å, b = 4.8537 Å, c = 5.5276 Å, α = γ = 90 °, and β = 104.264 °. Three different models were constructed according to the O/Ta ratios of the deposited Ta_2O_5 films. The microscopic band gaps, partial density of states (PDOS) and charge density difference were calculated using the first-principle pseudopotential method and the program of CASTEP (Cambridge Serial Total Energy Package) was performed [12-14]. The energy cutoff was set at 340 eV and the k-point grid was set to 3×3×3.

3. Results and discussion

Fig. 1 shows the transmittance spectra, refractive indices and extinction coefficients of the films. Fig. 1(a) illustrates that all the optical transmittance increases after annealing, which can be attributed to the decrease of absorption. In addition, Fig. 1(a) reveals that the transmittance curves shift to the short wavelength after annealing, indicating the decrease of the film thickness. Fig. 1(b) demonstrates that both the refractive index and extinction coefficient of A1 are higher than those of A2. After annealing, the refractive indices increase and the extinction coefficients decrease for both the films. Moreover, it should be noted that the extinction coefficients are too small to be determined when the wavelength is higher than 600 nm.

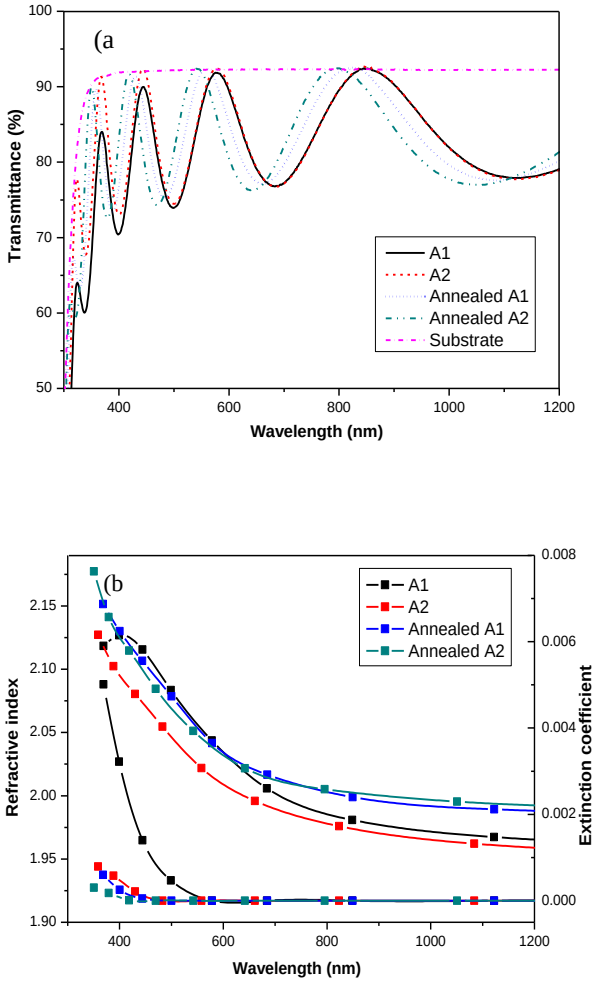

Fig. 1. Transmittance spectra, refractive indices and extinction coefficients of the films

High-resolution XPS is used to obtain the chemical composition of the films, as is shown in Fig. 2. The spectra of the surface (0 nm) in Fig. 2(a) reveal $4f_{7/2}$ and $4f_{5/2}$ peaks at 26.1 eV and 28.0 eV, which shows the composition of the films is Ta^{5+} [15]. For comparison, the spectra at 10 nm beneath the surface are also detected by XPS. Apart from $4f_{7/2}$ and $4f_{5/2}$ peaks, another two peaks are presented in Fig. 2(b) at 21.8 eV and 23.5 eV, indicating the existence of Ta^{2x+} [16]. It is probably due to the fact that the sputtering by Ar ions preferentially removes oxygen from Ta_2O_5. Therefore, the O/Ta ratios are estimated from the 0 nm XPS peak areas together with the relative sensitivity factors. The O/Ta ratios of A1 and A2 are 2.44 and 2.47, respectively. After annealing, both the O/Ta ratios of the films increase to 2.50.

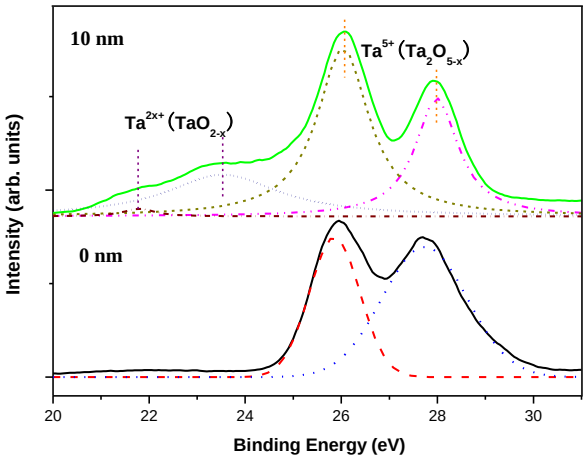

Fig. 2. Typical XPS narrow scan of Ta4f of the films

As is shown in Fig. 1, the extinction coefficients of all the films are very difficult to detect accurately. It is suggested that the optical absorption is not a proper parameter to evaluate the film absorption in this study. Therefore, the STL method is used to measure the weak absorption of the samples because it is much more sensitive. Ten sites on a line are detected on the films, and each site is about 100 μm. Fig. 3 illustrates that the average absorption of A1 and A2 is very high, which are 96.0 ppm and 87.5 ppm, respectively. After annealing, the absorption of A1 and A2 reduces to 49.7 ppm and 50.1 ppm, which decreases by 48.2% and 42.7%, respectively. The LIDT results of the films are shown in Fig. 4. It represents that the annealing gives rise to the LIDT. The LIDT of annealed A1 and annealed A2 increase by 62.2% and 54.7%, respectively, compared with the initial LIDT.

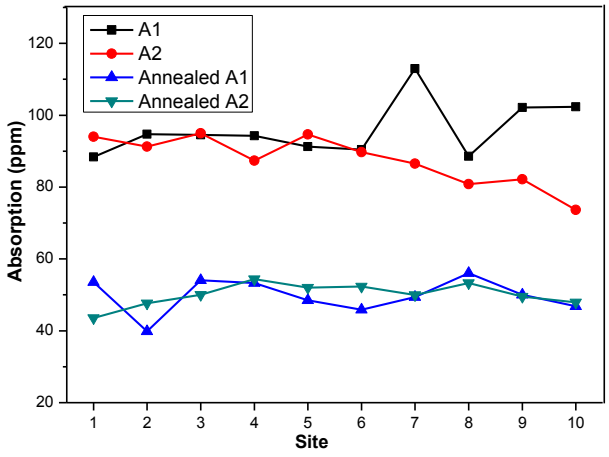

Fig. 3. Weak absorption of the films

At present the microscopic band gaps can not be estimated by the optical test, or say that the accuracy of the test measurement is too low to obtain the results. Therefore, the calculation based on the first-principle pseudopotential method is used to estimate the microscopic band gaps in this study. According to the O/Ta ratios detected by XPS results, three different Ta_2O_5 models are constructed in Fig. 5: a perfect unit cell, a 2×2×2 supercell with an oxygen vacancy and a 2×2×1 supercell with an oxygen vacancy. The theoretical O/Ta ratios of these models are 2.50, 2.47 and 2.44, respectively. Fig. 6 shows the calculated microscopic band gaps, which are 2.54 eV, 0.91 eV and 0.69 eV, respectively. It shows that the microscopic band gaps decrease by 64.2% and 72.8% when the O/Ta ratios decrease slightly from 2.50 to 2.47 and 2.44, respectively. It indicates that the oxygen vacancy significantly decreases the microscopic band gaps. According to Figs. 6(b) and 6(c), this decrease is mainly due to the generation of a defect level in the energy gap. The PDOS of Ta and O in Ta_2O_5 are shown in Fig. 7. It demonstrates the contribution of 5*d*, 5*p* and 6*s* orbitals of Ta, and 2*s*, 2*p* orbitals of O. The upper subband of the valence band is formed by 2*p* orbital of oxygen with partly contribution of Ta5*d*, while the conduction band is formed mostly by Ta5*d* state with an addition of O2*p* state. Moreover, it is clearly seen from Fig. 7(a) that the defect level in the energy gap caused by oxygen vacancy is mostly formed by 5*d* state of tantalum. Fig. 8 illustrates the typical charge density difference in the (010) plane of the perfect 2×2×1 supercell and the 2×2×1 supercell with an oxygen vacancy. Fig. 8(a) shows that the contour lines of charge density difference of Ta and O are overlapped, indicating the strong interaction and obvious characteristic of covalent bond. Fig. 8(b) shows that the charge density difference of the Ta around the oxygen vacancy decreases, which indicates that the covalent interaction becomes weaker.

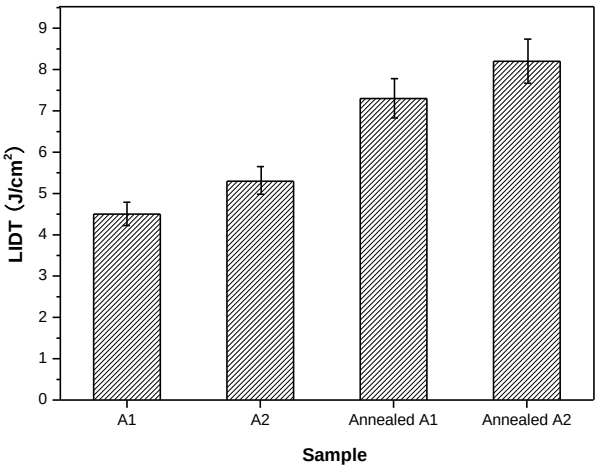

Fig. 4. LIDT results of the films

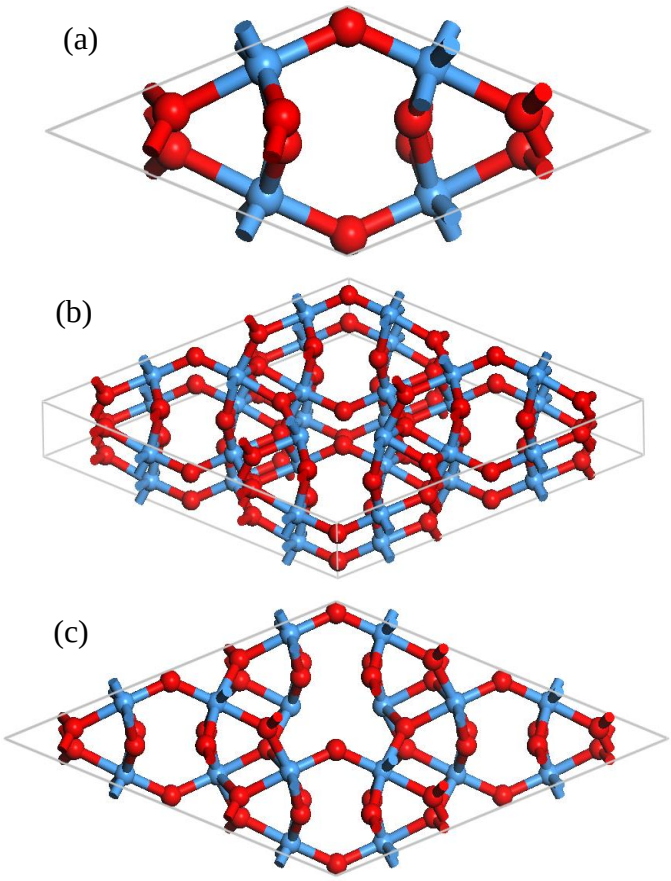

Fig. 5. Structure models of (a) perfect unit cell, (b) 2×2×2 supercell with an oxygen vacancy and (c) 2×2×1 supercell with an oxygen vacancy. (The red and blue spheres represent O and Ta atoms, respectively)

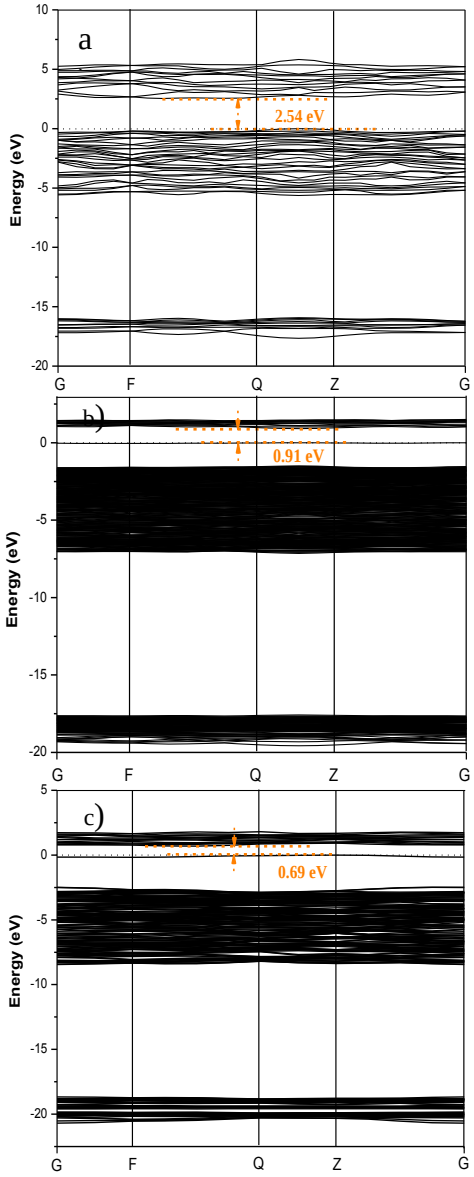

Fig. 6. Calculated microscopic band gaps of (a) perfect unit cell, (b) 2×2×2 supercell with an oxygen vacancy and (c) 2×2×1 supercell with an oxygen vacancy

From the above experimental and simulated results, it is found that the LIDT shares the same trend with the microscopic band gaps. With the increase of O/Ta ratios from 2.44 (A1) and 2.47 (A2) to 2.50 (annealed films), the LIDT increases by 62.2% and 54.7%, whereas the microscopic band gaps increase by 268% and 160%, respectively, compared to the initial value. This significant increase in the microscopic band gaps is attributed to the removal of the defect level in the energy gap. It indicates that the microscopic band gap is an effective parameter to evaluate the LIDT, and the PDOS and charge density difference may be beneficial to explore the underlying causes of the damage. It can be explained by the fact that the 1064 nm laser damage of films is influenced strongly by the microdefect or the nanodefect, thus the microscopic properties of the nano-area and even smaller area play an important role on the laser damage initiation.

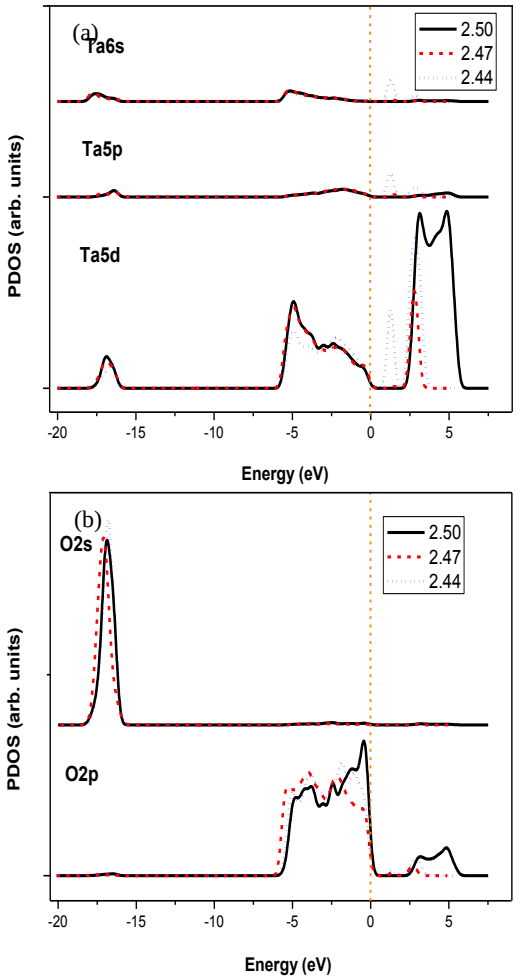

Fig. 7. PDOS of (a) Ta and (b) O in Ta_2O_5

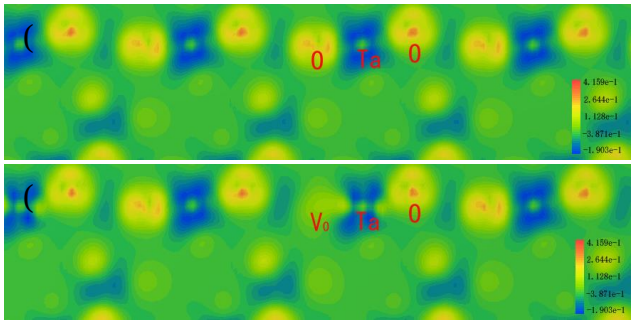

Fig. 8. Charge density difference of (a) perfect 2×2×1 supercell and (b) 2×2×1 supercell with an oxygen vacancy (V_o)

4. Conclusions

In summary, Ta_2O_5 films are prepared by electron beam evaporation and different models are constructed according to the experimental obtained O/Ta ratios. It shows that the oxygen vacancy significantly decreases the microscopic band gaps. The LIDT shares the same trend with the microscopic band gaps. With the O/Ta ratios increase from 2.44 and 2.47 to 2.50, the LIDT increases by 62.2% and 54.7%, whereas the microscopic band gaps increase by 268% and 160%, respectively. This significant increase in the microscopic band gaps is attributed to the removal of the defect level in the energy gap.

Acknowledgement

This work is supported by "the Fundamental Research Funds for the Central Universities (2015XKMS065)" and "the Six Talent Peaks Project in Jiangsu Province (2015-XCL-009)".

References

[1] Y. Zhao, Y. Wang, H. Gong, J. Shao, Z. Fan, Appl. Surf. Sci. **210**, 353 (2003).
[2] C. R. Wolfe, M. R. Kozlowski, J. H. Campbell, F. Rainer, A. J. Morgan, R. P. Gonzales, Proc. SPIE **1438**, 360 (1989).
[3] Z. Liu, S. Chen, P. Ma, Y. Wei, Y. Zheng, F. Pan, H. Liu, G. Tang, Opt. Express **20**, 854 (2012).
[4] J. H. Sun, B. H. Wu, H. B. Jia, D. Wu, Y. Xu, Opt. Lett. **37**, 4095 (2012).
[5] C. Xu, D. Li, H. Fan, J. Deng, J. Qi, P. Yi, Y. Qiang, Thin Solid Films, **580**, 12 (2015).
[6] C. Xu, D. Li, J. Ma, Y. Jin, J. Shao, Z. Fan, Opt. Laser. Technol. **40**, 545 (2008).
[7] C. Xu, J. Jia, D. Yang, H. Fan, Y. Qiang, J. Liu, G. Hu, D. Li, J. Appl. Phys. **116**, 053102 (2014).
[8] C. Xu, S. Yang, J. Wang, J. Liu, H. Ma, Y. Qiang, J. Liu, D. Li, C. Tao, Chin. Phys. Lett. **29**, 084207 (2012).
[9] H. He, X. Li, S. Fan, J. Shao, Y. Zhao, Z. Fan, Proc. SPIE **5991**, 59912F (2005).
[10] ISO 11254-1:2000: lasers and laser-related equipment-determination of laser-induced damage threshold of optical surfaces. Part 1. 1-on-1 test.
[11] H. Hu, Z. Fan, F. Luo, Appl. Opt. **40**, 1950 (2001).
[12] V. V. Atuchin, J.-C. Grivel, A. S. Korotkov, Z. Zhang, J. Solid State Chem. **181**, 1285 (2008).
[13] V. A. Pustovarov, T. V. Perevalov, V. A. Gritsenko, T. P. Smirnov, A. P. Yelisseyev, Thin Solid Films **519**, 6319 (2011).
[14] M. C. Payne, M. P. Teter, D. C. Allan, T. A. Arias, J. D. Joannopoulos, Rev. Modern Phys. **64**, 1045 (1992).
[15] V. V. Atuchin, J.-C. Grivel, Z. Zhang, Chem. Phys. **360**, 74 (2009).
[16] M. V. Ivanov, T. V. Perevalov, V. S. Aliev, V. A. Gritsenko, V. V. Kaichev, J. Appl. Phys. **110**, 024115 (2011).

*Corresponding author: xucheng@cumt.edu.cn